J|A|C|S
ARTICLES
Published on Web 11/24/2004

Nature of Urea−Fluoride Interaction: Incipient and Definitive Proton Transfer

Massimo Boiocchi,[‡] Laura Del Boca,[†] David Esteban Gómez,[†] Luigi Fabbrizzi,*[,†] Maurizio Licchelli,[†] and Enrico Monzani[†]

Contribution from the Dipartimento di Chimica Generale, Università di Pavia, via Taramelli 12, 27100 Pavia, Italy, and Centro Grandi Strumenti, Università di Pavia, via Bassi 10, 27100 Pavia, Italy

Received July 7, 2004; E-mail: luigi.fabbrizzi@unipv.it

Abstract: 1,3-bis(4-nitrophenyl)urea (**1**) interacts through hydrogen bonding with a variety of oxoanions in an MeCN solution to give bright yellow 1:1 complexes, whose stability decreases with the decreasing basicity of the anion (CH_3COO^- > $C_6H_5COO^-$ > $H_2PO_4^-$ > NO_2^- > HSO_4^- > NO_3^-). The [Bu_4N][**1**·CH_3COO] complex salt has been isolated as a crystalline solid and its molecular structure determined, showing the formation of a discrete adduct held together by two N−H···O hydrogen bonds of moderate strength. On the other hand, the F^- ion first establishes a hydrogen-bonding interaction with **1** to give the most stable 1:1 complex, and then on addition of a second equivalent, induces urea deprotonation, due to the formation of HF_2^-. The orange-red deprotonated urea solution uptakes carbon dioxide from air to give the tetrabutylammonium salt of the hydrogencarbonate H-bond complex, [Bu_4N][**1**·HCO_3], whose crystal and molecular structures have been determined.

Introduction

The design of artificial receptors capable of selective interactions with electrically charged substrates stays at the basis of many important subdisciplines of supramolecular chemistry, which investigate a variety of functions, including recognition, sensing, catalysis, and carrier-mediated transport across membranes.[1] In a historical prospect, supramolecular chemistry developed with the synthesis of neutral receptors (cyclic and polycyclic poly-ethers)[2,3] suitable for the selective interaction with alkali metal cations. Reversibility of the cation−donor atom interaction is an essential requirement for the above-mentioned functions to take place. In a broad sense, these studies represented an extension to *s*-block metals of the concepts and principles of classical coordination chemistry, which had developed much earlier from the study of the interactions of *d*-block cations with neutral receptors (ligands) containing amine groups (even if the metal−amine interaction may be irreversible). A coordination chemistry of anions has developed more recently based on electrostatic and dipolar interactions between the receptor and the substrate.[4,5] In particular, neutral receptors exist also for anions; most of them contain −NH fragments which act as hydrogen bond donors for the anion.[6] In contrast to merely electrostatic interactions, H-bonds are directional, a feature which allows the design of receptors capable of differentiating between anions with different geometries and hydrogen-bonding requirements. As an example, seminal papers by Wilcox and Hamilton showed that urea is a good H-bond donor and an excellent receptor for Y-shaped anions, such as carboxylates, through the formation of two hydrogen bonds.[7,8] A variety of receptors containing one or more urea subunits have been designed and tested for anion recognition and sensing over the past years.[9] Moreover, selectivity is also related to the energy of the receptor−anion interaction; in this sense, strong H-bond interactions are established with anions containing the most electronegative atoms: F (fluoride) and O (carboxylates, inorganic oxoanions). According to a recent view, "all hydrogen bonds can be considered as incipient proton-transfer reactions, and for strong hydrogen bonds, this reaction can be in a very advanced state".[10] Thus, for a given −NH-containing receptor (the acid), selectivity should be mainly related to the basicity of the A^- anion (i.e., to the pK_a value of the conjugated acid HA); the higher anion basicity, the stronger the hydrogen-bonding interaction. Solvent cannot be water or any other hydrogen bond-forming medium (e.g., alcohols) since they would compete successfully with the receptor for the anion. Thus, aprotic solvents of varying polarity are currently employed in anion recognition studies based on H-bonds (e.g., $CHCl_3$, MeCN, and DMSO).

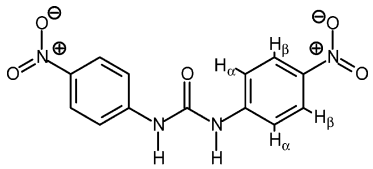

1

[†] Dipartimento di Chimica Generale.
[‡] Centro Grandi Strumenti.

(1) Lehn, J.-M. *Supramolecular Chemistry, Concepts and Perspectives*; VCH: Weinheim, Germany, 1995.
(2) Pedersen, C. J. *J. Am. Chem. Soc.* **1967**, *89*, 7017−7036.
(3) Dietrich, B.; Lehn, J.-M.; Sauvage, J.-P. *Tetrahedron Lett.* **1969**, *34*, 2885−2888.
(4) *Supramolecular Chemistry of Anions*; Bianchi, A., Bowman-James, K., García-España, E., Eds.; Wiley-VCH: New York, 1997.
(5) Beer, P. D.; Gale, P. A. *Angew. Chem., Int. Ed.* **2001**, *40*, 486−516.
(6) Gale, P. A. *Coord. Chem. Rev.* **2003**, *240*, 1−226.

10.1021/ja045936c CCC: $27.50

In this context, we were interested in investigating in detail the nature of the interaction of the urea subunit with anions. In particular, we chose the derivative **1**, 1,3-bis(4-nitrophenyl)-urea. 4-Nitrophenyl substituents were appended to the urea moiety for two main reasons. (i) Presence of $-NO_2$ electron-withdrawing substituents is expected to enhance the acidity and, as a consequence, the H-bond donor properties of the receptor. (ii) The optical properties of the chromogenic nitrophenyl fragment may be altered following receptor−anion interaction, thus providing colorimetric and spectral sensing of the recognition event. Indeed, it has been shown that even simple chromophores, containing hydrogen-bonding donor groups, can operate as efficient colorimetric sensors for the naked-eye detection of anions.[11]

Experimental Section

General Procedures and Materials. All reagents for the syntheses were purchased by Aldrich/Fluka and used without further purification. UV−vis spectra were recorded on a Varian CARY 100 spectrophotometer, with a quartz cuvette (path length = 1 cm), and on a Hewlett-Packard 8452A spectrophotometer, with a quartz cuvette (path length = 10 cm). The cell holder was thermostated at 25.0 °C, through circulating water. ^{1}H NMR spectra were obtained on a Bruker AVANCE 400 spectrometer (400 MHz), operating at 9.37 T. Spectrophotometric titrations were performed on $2-5 \times 10^{-5}$ and 1.0×10^{-6} M solutions of **1** and in MeCN (polarographic grade). Typically, aliquots of a fresh alkylammonium salt standard solution of the envisaged anion (CH_3COO^-, $C_6H_5COO^-$, $H_2PO_4^-$, NO_2^-, HSO_4^-, NO_3^-, F^-, or Cl^-) were added, and the UV−vis spectra of the samples were recorded. All spectrophotometric titration curves were fitted with the HYPERQUAD program.[12] Care was taken that in each titration, the p parameter (p = [concentration of complex]/[maximum possible concentration of complex]) was lower than 0.8, a condition required for the safe determination of a reliable equilibrium constant.[13] ^{1}H NMR titrations were carried out on DMSO-d_6 solution, at a higher concentration of **1** (5×10^{-3} M).

Synthesis of 1,3-Bis(4-nitrophenyl)urea (1). 4-Nitrophenylisocyanate (0.027 g, 0.163 mmol) was added to a solution of 4-nitroaniline (0.022 g, 0.163 mmol) in dry dioxane (10 mL), in a round flask filled with argon. The mixture was heated at 100 °C under magnetic stirring for 24 h. During the reaction, a yellow precipitate formed, which was collected by filtration, washed with water, and dried in vacuo. The yellow solid (0.044 g, 89%) is air stable, soluble in DMSO, partially soluble in acetonitrile, and insoluble in all other common solvents: ^{1}H NMR (DMSO-d_6) δ_H 8.22 (d, 2H, H$_\beta$), 7.73 (d, 2H, H$_\alpha$), 9.70 (s, 2H, NH), coupling constants determined for an AA′MM′ system $J_{H\alpha,H\beta} = J_{H\beta,H\alpha} = 8$ Hz; IR (Nujol, cm^{-1}) ν 1741 (C═O), 1577 ν(N−O), 1461 $\nu_{as}(NO_2)$, 1301 $\nu_s(NO_2)$, 3365, 3339 ν_{as},ν_s(N−H), 1498, 1249 δ_{as},δ_s-(N−H).

X-ray Crystallographic Studies. Diffraction data were collected at room temperature by means of an Enraf-Nonius CAD4 four-circle diffractometer, working with graphite-monochromatized Mo Kα X-radiation (λ = 0.71073 Å). Crystal data for the [Bu$_4$N][**1**·CH$_3$COO] and [Bu$_4$N][**1**·HCO$_3$]·2H$_2$O complex salts are reported in Table 1.

Data reductions (including intensity integration, background, Lorentz, and polarization corrections) were performed with the WinGX package.[14] Absorption effects were evaluated with the psi-scan method,[15] and absorption correction was applied to the data (min/max transmission factors for the crystals were 0.922/0.968 and 0.910/0.971). Crystal structures were solved by direct methods (SIR 97)[16] and refined by full-matrix least-squares procedures on F^2 using all reflections (SHELXL 97).[17] Anisotropic displacement parameters were refined for all non-hydrogen atoms. Hydrogens bonded to carbon atoms were placed at calculated positions with the appropriate AFIX instructions and refined using a riding model; hydrogens bonded to the N(1) and N(3) amines, as well as those belonging to water molecules and the hydrogencarbonate anion, were located in the ΔF map and refined by restraining the X−H distance to be 0.89 ± 0.02 Å.

Table 1. Crystal Data for the Complex Salts, [Bu$_4$N][**1**·CH$_3$COO] and [Bu$_4$N][**1**·HCO$_3$]·2H$_2$O

	[Bu$_4$N][**1**·CH$_3$COO]	[Bu$_4$N][**1**·HCO$_3$]·2H$_2$O
formula	$C_{31}H_{49}N_5O_7$	$C_{30}H_{51}N_5O_{10}$
M	603.75	641.76
color	deep yellow	deep yellow
dimension (mm)	0.70 × 0.50 × 0.35	0.70 × 0.50 × 0.35
crystal system	monoclinic	monoclinic
space group	$P2_1/c$ (no. 14)	$P2_1/c$ (no. 14)
a [Å]	10.0827(17)	9.6592(25)
b [Å]	20.4341(23)	18.2763(14)
c [Å]	17.2817(48)	19.8024(27)
β [deg]	106.067(22)	91.517(10)
V [Å^3]	3421.5(12)	3494.4(12)
Z	4	4
ρ_{calcd} [g cm^{-3}]	1.172	1.220
μ Mo Kα [mm^{-1}]	0.083	0.092
scan type	$\omega - 2\theta$ scans	$\omega - 2\theta$ scans
θ range [deg]	2−26	2−26
measured reflns	7094	14221
unique reflns	6700	6859
R_{int}[a]	0.0331	0.0735
strong data [$I_O > 2\sigma(I_O)$]	2198	2429
R1, wR2 (strong data)[b]	0.0757, 0.1254	0.0600, 0.1102
R1, wR2 (all data)[b]	0.2425, 0.1794	0.1995, 0.1524
GOF[c]	0.980	0.946
refined parameters	395	431
max/min residuals [e Å^{-3}]	0.15/−0.14	0.19/−0.15

[a] $R_{int} = \sum|F_o^2 - F_o^2(\text{mean})|/\sum F_o^2$. [b] $R1 = \sum ||F_o| - |F_c||/\sum |F_o|$, wR2 = $[\sum [w(F_o^2 - F_c^2)^2]/[\sum w(F_o^2)^2]]^{1/2}$, where $w = 1/[\sigma^2F_o^2 + (aP)^2 + bP]$ and $P = [(\max (F_o^2,0) + 2F_c^2]/3$. [c] GOF = $\{\sum[w(F_o^2 - F_c^2)^2]/(n - p)\}^{1/2}$, where n is the number of reflections and p the total number of refined parameters.

Results and Discussion

The interaction of receptor **1** with the Y-shaped anion CH_3COO^- was investigated in an MeCN solution through spectrophotometric titration experiments. In particular, a standard solution of [Bu$_4$N]CH$_3$COO was added stepwise to a 4×10^{-5} M solution of **1** at 25 °C. Upon acetate addition, the pale yellow solution of **1** took a bright yellow color, as shown in the picture in Figure 1.

Figure 2 shows the family of spectra taken in the course of the titration. Upon addition of CH_3COO^-, the band at 345 nm progressively decreases, while a new band at 370 nm forms and develops. Presence of two sharp isosbestic points at 262 and 354 nm indicates that only two species coexist at the equilibrium. The profile of the intensities of the bands at 345

(7) Smith, P. J.; Reddington, M. V.; Wilcox, C. S. *Tetrahedron Lett.* **1992**, *41*, 6085−6088.
(8) Fan, E.; van Arman, S. A.; Kincaid, S.; Hamilton, A. D. *J. Am. Chem. Soc.* **1993**, *115*, 369−370.
(9) Fitzmaurice, R. J.; Kyne, G. M.; Douheret, D.; Kilburn, J. D. *J. Chem. Soc., Perkin Trans. 1* **2002**, 841−864.
(10) Steiner, T. *Angew. Chem., Int. Ed.* **2002**, *41*, 48−76.
(11) Miyaji, H.; Sessler, J. L. *Angew. Chem., Int. Ed.* **2001**, *40*, 154−157.
(12) Gans, P.; Sabatini, A.; Vacca, A. *Talanta* **1996**, *43*, 1739−1753.
(13) Wilcox, C. S. *Frontiers in Supramolecular Chemistry and Photochemistry*; VCH: Weinheim, Germany, 1991; pp 123−143.
(14) Farrugia, L. J. *J. Appl. Crystallogr.* **1999**, *32*, 837−838.
(15) North, A. C. T.; Phillips, D. C.; Mathews, F. S. *Acta Crystallogr.* **1968**, *A24*, 351−359.
(16) Altomare, A.; Burla, M. C.; Camalli, M.; Cascarano, G. L.; Giacovazzo, C.; Guagliardi, A.; Moliterni, A. G. G.; Polidori, G.; Spagna, R. *J. Appl. Crystallogr.* **1999**, *32*, 115−119.
(17) Sheldrick, G. M. *SHELX97: Programs for Crystal Structure Analysis*; University of Göttingen: Göttingen, Germany, 1997.

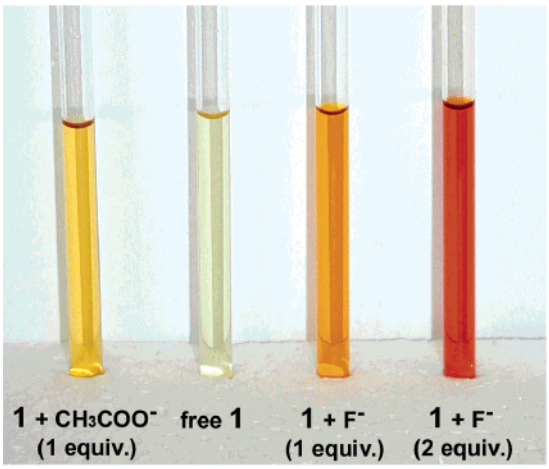

Figure 1. Color changes observed with the addition of anions to an MeCN solution of **1**.

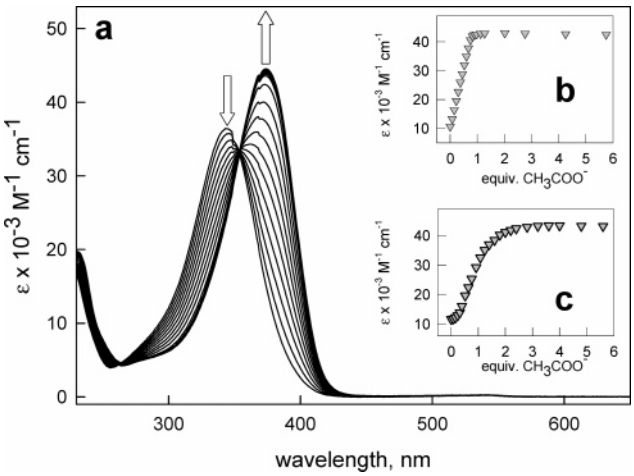

Figure 2. (a) Family of spectra taken in the course of the titration of a 2.6 $\times$ 10^{-5} M solution in **1** with a standard solution of $[Bu_4N]CH_3COO$ at 25 °C. (b) Titration profile for the 2.6 $\times$ 10^{-5} M MeCN solution $\times$in **1**, which indicates the formation of a 1:1 adduct [**1**·CH_3COO]. (c) Titration profile for a 1.0 $\times$ 10^{-6} M solution in **1**, from which the association constant was determined, log K = 6.61 $\pm$ 0.09.

(decreasing) and 370 nm (increasing), shown in Figure 2a, indicates a 1:1 stoichiometry for the receptor−acetate interaction. Data can be interpreted on the basis of the following equilibrium: **1** + CH_3COO^- ⇆ [**1**·CH_3COO]$^-$, in which [**1**·CH_3COO]$^-$ represents the receptor−anion complex. However, the curvature in the titration profile reported in graph a is too steep to allow a safe determination of the binding constant. In particular, the p parameter (p = [concentration of complex]/[maximum possible concentration of complex]) was found higher than 0.8, a condition which does not permit the determination of a reliable equilibrium constant.[13] Thus, titration was carried out on a distinctly more diluted solution (1.0 $\times$ 10^{-6} M; see the smoother titration profile in inset c). In these conditions, the p parameter was lower than 0.8, and a reliable value of the association constant could be determined through nonlinear least-squares treatment of the titration profile: log K = 6.61 $\pm$ 0.01.

The interaction of receptor **1** with acetate (used as tetrabutylammonium salt) was investigated by ^{1}H NMR spectroscopy. However, the limited solubility of **1** prevented the recording of well-resolved spectra in CD_3CN. Thus, ^{1}H NMR titration experiments were carried out in DMSO-d_6, where **1** presents a

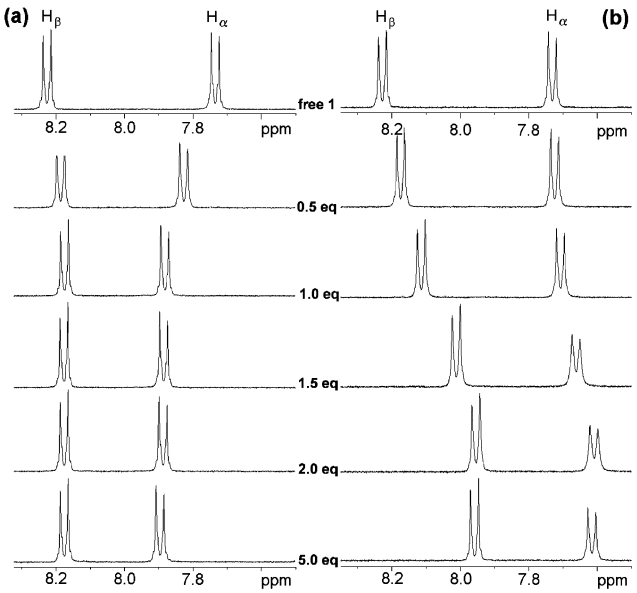

Figure 3. Titration of a 5 $\times$ 10^{-3} M solution of **1** in DMSO-d_6 with (a) CH_3COO^- and (b) F^-.

higher solubility. However, apart from the different resolution, spectra recorded in CD_3CN and in DMSO-d_6 exhibited similar patterns. In particular, a 5 $\times$ 10^{-3} M DMSO-d_6 solution in **1** was titrated with CH_3COO^-, which was added stepwise up to 5 equiv. Figure 3a shows the NMR spectra obtained in the course of the titration and illustrates the spectral shifts of the aromatic protons of the phenyl rings linked to the urea moiety, H_α and H_β, with the addition of acetate. Spectra indicate the formation of a discrete H-bond complex. In fact, two effects are expected to derive from the hydrogen bond formation between the urea subunit and the anion. (i) The increase of electron density in the phenyl rings, with a through-bond propagation; this causes a shielding effect and should promote an upfield shift. (ii) The polarization of the C−H bonds, induced by a through-space effect, electrostatic in origin; in particular, the partial positive charge created onto the proton causes a deshielding effect and promotes a downfield shift. The latter effect is expected to vanish at higher distances and should therefore operate only on the C−H_α bond. In fact, in the case of C−H_α proton, the electrostatic effect dominates, and a progressive downfield shift is observed, which stops after a 1 equiv addition. On the other hand, C−H_β protons feel neither the anion-induced electrostatic effect nor the C−H_α polarization effect, thus being affected only by the through-bond effect, which induces a moderate upfield shift. Also in this case, shift stops after a 1 equiv addition of acetate.

The above evidence points toward the formation of a [**1**·CH_3COO]$^-$ H-bond complex. The nature of such a complex was definitively demonstrated through X-ray diffraction studies. In particular, on slow evaporation of an MeCN solution containing equimolar amounts of **1** and $[Bu_4N]CH_3COO$, crystals of a salt of formula $[Bu_4N]$[**1**·CH_3COO], suitable for crystallographic studies, were obtained. The ORTEP diagram of the complex salt is shown in Figure 4.

It is observed that the acetate ion establishes two directional H-bonds with the two −NH fragments of the urea subunit. To our knowledge, this is the first crystallographic report in which a distinct urea subunit interacts with an acetate ion, in a discrete

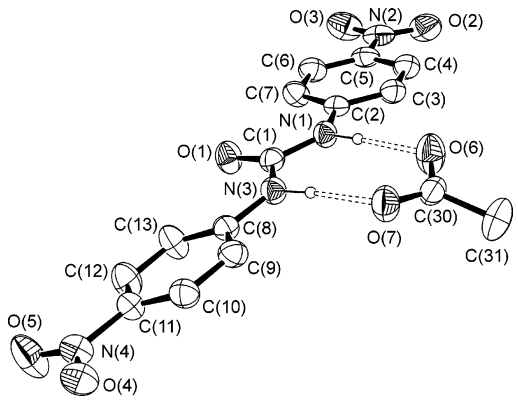

Figure 4. ORTEP view of the $[\mathbf{1}\cdot CH_3COO]^-$ complex (thermal ellipsoids are drawn at the 30% probability level; only H atoms involved in intermolecular hydrogen bonds are drawn). Tetrabutylammonium ion has been omitted for clarity. Dashed lines indicate the hydrogen-bond interactions.

Table 2. Geometrical Features of the NH···O Interactions with the Y-Shaped Anions in $[\mathbf{1}\cdot CH_3COO]^-$ and $[\mathbf{1}\cdot HCO_3]^-\cdot H_2O$[a]

donor group	anion	D···A (Å)	H···A (Å)	D–H···A (deg)	acceptor atom
N(1)−H(1N)	CH_3COO^-	2.693(5)	1.797(28)	170.9(26)	
	HCO_3^-	2.811(4)	1.929(23)	166.8(21)	O(6)
N(3)−H(3N)	CH_3COO^-	2.770(5)	1.852(30)	174.4(27)	
	HCO_3^-	2.790(4)	1.897(23)	169.7(20)	O(7)
O(8)−H(80)	HCO_3^-	2.617(4)	1.681(22)	171.5(21)	O(7′)
O(9)−H(90A)	HCO_3^-	2.982(4)	2.113(36)	162.1(26)	O(1″)
O(9)−H(90B)	HCO_3^-	2.908(4)	2.043(33)	160.2(29)	O(6)
O(10)−H(91A)	HCO_3^-	2.767(4)	1.863(26)	172.5(19)	O(9)
O(10)−H(91B)	HCO_3^-	3.069(4)	2.238(32)	152.9(25)	O(3‴)

[a] Features of the O−H···O interactions involving OH groups in $[\mathbf{1}\cdot HCO_3]^-\cdot H_2O$ are also reported. Symmetry codes: (′) = $-x + 1, -y + 1, -z$; (″) = $x + 1, y, z$; (‴) = $-x + 1, -y + 1, -z + 1$.

1:1 anionic complex. A report was given in which a urea fragment belonging to a metal-bound multidentate ligand interacted with acetate anions.[18] The N(urea)−O(acetate) distances in the $[\mathbf{1}\cdot CH_3COO]^-$ complex (2.69 and 2.77 Å) situate the interaction among "moderate" hydrogen bonds, whose nature is mainly electrostatic, according to Jeffrey's classification.[19] Significant bond distances and angles for the hydrogen-bonding interactions in the $[\mathbf{1}\cdot CH_3COO]^-$ complex are reported in Table 2. In the table, relevant data for the hydrogencarbonate complex of **1**, $[\mathbf{1}\cdot HCO_3]^-\cdot H_2O$, are also reported and to be discussed later.

Notice that the distances between the ortho protons nearest to the carbonyl oxygen [2.217(4) and 2.207(4) Å] are among the shortest observed for diarylureas.[20] These features suggest the presence of weak symmetrical CH···O interactions, satisfying the hydrogen bond acceptor ability of the carbonyl oxygen. Moreover, it has to be noted that the nitrophenyl substituents are not perfectly coplanar with the urea subunit: the two dihedral angles of the N−CO−N group are 7.4(2) and 11.2(3)°. Such a nonplanarity can be ascribed to crystal packing effects associated with the asymmetrical position of the tetrabutylammonium cation.

(18) Carcelli, M.; Ianelli, S.; Pelagatti, P.; Pelizzi, G. *Inorg. Chim. Acta* **1999**, *292*, 121−126.
(19) Jeffrey, G. A. *An Introduction to Hydrogen Bonding*; Oxford University Press: Oxford, 1997.
(20) Etter, M. C.; Urbañczyk-Lipkowska, Z.; Zia-Ebrahimi, M.; Panunto, T. W. *J. Am. Chem. Soc.* **1990**, *112*, 8415−8426.

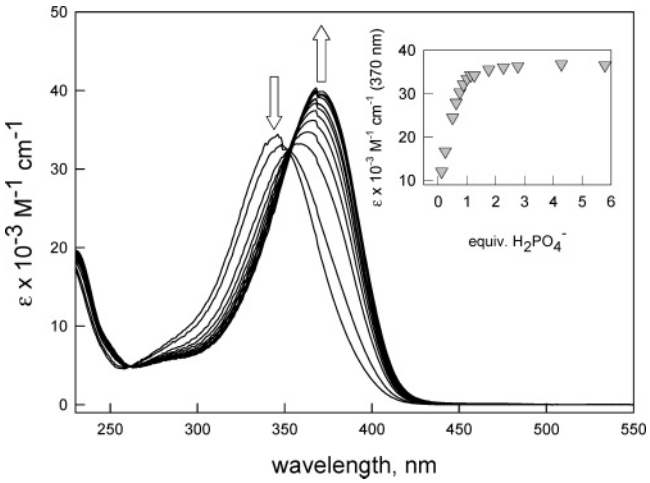

Figure 5. Family of spectra taken in the course of the titration of a 1×10^{-6} M MeCN solution in **1** with a standard solution of $[Bu_4N]H_2PO_4$ at 25 °C. Titration profiles (inset) indicate the formation of a 1:1 complex, $[\mathbf{1}\cdot H_2PO_4]$, to which a binding constant, $\log K = 5.37 \pm 0.01$, corresponds.

Table 3. Constants of the Complex Formation Equilibrium[a]

anion	log K[b]	ϵ (M^{-1} cm^{-1})
CH_3COO^-	6.61 (1)	42172 (370 nm)
$C_5H_6COO^-$	6.42 (1)	38249 (370 nm)
$H_2PO_4^-$	5.37 (1)	39406 (370 nm)
F^-[c]	log K_1= 7.38 (9)	20712 (370 nm)
	log K_2= 6.37 (12)	19324 (470 nm)
NO_2^-	4.33 (1)	27200 (370 nm)
HSO_4^-	4.26 (1)	28600 (370 nm)
NO_3^-	3.65 (5)	23300 (370 nm)
Cl^-	4.55 (1)	28700 (370 nm)

[a] In an MeCN solution at 25 °C: $\mathbf{1}$ + anion$^-$ ⇆ [**1**·anion]$^-$, and molar absorbances (ϵ) of the [**1**·anion]$^-$ H-bond complexes. [b] The value in parentheses is the uncertainty of the last figure. [c] The value of log K_1 refers to the H-bond complex formation; log K_2 refers to the receptor's deprotonation equilibrium: $[LH\cdot F]^- + F^- \leftrightarrows L^- + [HF_2]^-$.

The electronic rearrangement of receptor **1** following interaction with acetate is demonstrated also by IR spectra. In particular, the C═O stretching band of the urea fragment of **1** moves from 1742 to 1720 cm^{-1} in the $[\mathbf{1}\cdot CH_3COO]^-$ complex, indicating definite bond weakening. This reflects the acetate-induced increase of the electron density, which goes in part to populate the π^* orbital of the C═O fragment, reducing bond order.

Analogous investigations were carried out with a variety of oxoanions ($H_2PO_4^-$, NO_3^-, NO_2^-, HSO_4^-, and $C_6H_5COO^-$). In particular, an MeCN solution of **1** was titrated with a standard solution of the tetrabutylammonium salt of the chosen anion. In all cases, a new absorption band at ∼370 nm developed on titration, and sharp isosbestic points were observed in the recorded family of spectra. As an example, Figure 5 displays the spectra obtained on titration with $[Bu_4N]H_2PO_4$. Spectral features are the same as those observed for CH_3COO^-. Simply, the titration profile (inset) shows a smoother curvature, to which a smaller value of the binding constant corresponds ($\log K = 5.37 \pm 0.01$). Log K values and pertinent spectroscopic parameters for all investigated oxoanions are reported in Table 3.

^{1}H NMR titration experiments with oxoanions showed similar patterns as those observed with CH_3COO^-. The above evidence points toward the formation of a 1:1 adduct held together by two hydrogen bonds, each one involving an −NH fragment of

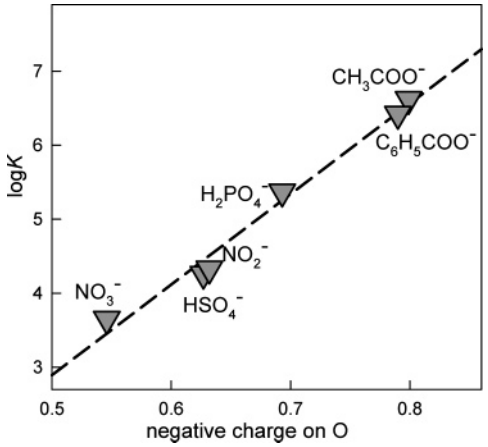

Figure 6. Linear relationship between the log *K* value of the complexation equilibrium (**1** + $X^- \leftrightarrows$ [**1**·X]$^-$) in MeCN and the average negative charge on the oxygen atom of the oxoanion, X^-. Partial charges were calculated through an ab initio method.

1 and an oxygen atom of the oxoanion. The sequence of the log *K* values ($CH_3COO^- > C_6H_5COO^- > H_2PO_4^- > NO_2^- > HSO_4^- > NO_3^-$) should reflect the decreasing intrinsic basicity of the anion. In particular, a reasonably linear correlation was observed between log *K* and the average negative charge on the oxygen atoms of each oxoanion, as calculated through an ab initio method (see Figure 6).

The higher the negative charge, the higher the H-bond acceptor tendencies of the anion. The existence of such a relationship points toward the electrostatic nature of the receptor−oxoanion interaction and rules out any geometrical effect on the binding (e.g., matching of the distance of the N atoms of the urea subunit and the distance of the O atoms of the oxoanion).

Fluoride displays a more intricate behavior. Figure 7a shows the complete family of spectra obtained during the titration of a 1.0×10^{-6} M solution of **1** in MeCN with [Bu_4N]F; it is seen that the band at 345 nm decreased, while a band at 370 nm formed and developed, as previously noticed for oxoanions. In particular, the band at 370 nm reached its limiting value after the addition of 1 equiv of F^-. This behavior is illustrated in Figure 7c. However, when approaching 1 equiv of F^-, a new band began to form at 475 nm. The band at 475 nm reached a limiting value after the addition of 2 equiv of F^- (see Figure 7d), while the solution took an orange-red color (see Figure 1). The titration profiles, shown in insets c and d of Figure 7, clearly indicate the presence of two distinct steps.

In fact, best fitting of the overall titration data was obtained by assuming the existence of two stepwise equilibria, in which (i) **1** interacts with F^- to give [**1**·F]$^-$ and (ii) the [**1**·F]$^-$ complex interacts with another F^- ion. Constants for the two stepwise equilibria, as calculated through nonlinear least-squares treatment of spectrophotometric titration data, were log $K_1 = 7.38 \pm 0.09$ (**1** + F^-) and log $K_2 = 6.37 \pm 0.12$ ([**1**·F]$^-$ + F^-). The distribution diagram of the three species present at the equilibrium in the course of the titration with F^-, calculated by the

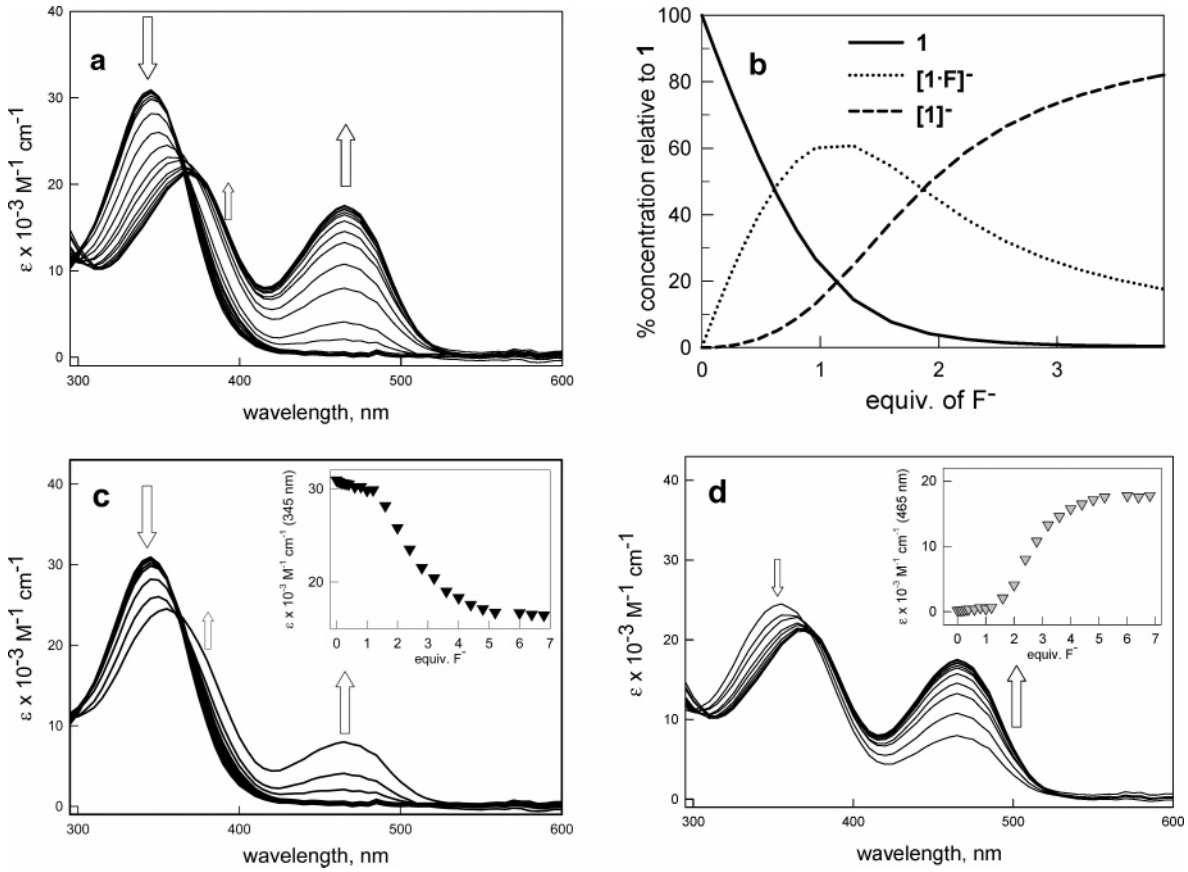

Figure 7. (a) Family of spectra taken in the course of the titration of a 1.0×10^{-6} M MeCN solution ×in **1** with a standard solution of [Bu_4N]F at 25 °C. (b) Distribution diagram of the species present at the equilibrium, which has been calculated for a 1.0×10^{-6} M solution of **1** in MeCN titrated with [Bu_4N]F. The solid line refers to the uncomplexed ligand **1**, the dashed line to the H-bond complex [**1**·F]$^-$, and the dotted line to the deprotonated form of **1**. (c) Addition of up to 1.0 equiv of F^-. (d) Addition of 1.0−5 equiv of F^-. Insets: titration profiles of the band at 345 nm, which corresponds to the H-bond adduct [**1**·F]$^-$ (c), and of the band at 475 nm, which corresponds to the deprotonated form of **1** (d).

Scheme 1. Charge Transfer Transition Occurring in the Deprotonated Form of **1**

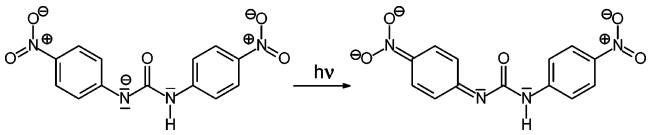

HYPERQUAD software package[12] from pertinent log *K* values for a 1.0×10^{-6} M solution of **1**, is shown in Figure 7b. The three species are (i) the receptor **1**, (ii) the product of the first equilibrium, presumably the $[\mathbf{1}\cdot F]^-$ H-bond complex, which reaches its maximum concentration (~60%) with addition of 1 equiv of F^-, and (iii) the product of the second equilibrium, whose nature has to be ascertained and whose concentration tends to 100%, with the addition of excess F^-.

A DMSO-d_6 solution of **1** was titrated with $[Bu_4N]F$, and corresponding ^1H NMR spectra are shown in Figure 3b. Different patterns are observed in the titration ranges of 0−1 and 1−2 equiv. In fact, $C-H_\beta$ protons undergo upfield shift in both the 0−1 and 1−2 equiv ranges, while $C-H_\alpha$ protons are insensitive to the first equivalent addition but undergo upfield shift with the addition of the second equivalent of fluoride. In any case, the shift is stopped after addition of the second equivalent. This state of affairs can be accounted for by hypothesizing that the first added F^- establishes H-bond interaction with the urea subunit of **1**. On addition of the second fluoride ion, deprotonation of one −NH fragment takes place, which brings electron density onto the phenyl rings according to a through-bond mechanism, thus increasing the shielding of H_α nuclei and inducing upfield shift. Notice also that, in the deprotonated form, the polarization effect is no longer present since the anion does not remain in proximity to the receptor. Thus, it is suggested that the first added F^- interacts with **1** through hydrogen bonding, while the second F^- induces the deprotonation of one −NH fragment of the urea subunit, with formation of the $[HF_2]^-$ ion, as illustrated by the equation below (LH = **1**):

$$[LH\cdot F]^- + F^- \leftrightarrows L^- + [HF_2]^- \qquad (1)$$

The deprotonated species (L^-) is a push−pull chromophore, which undergoes an optical charge-transfer transition, as illustrated in Scheme 1. This low-energy transition is responsible for the appearance of the band at 475 nm and for the development of the orange-red color.

Due to the rather large log K_2 value, which characterizes the proton transfer equilibrium (eq 1), the deprotonated form of the receptor forms quite early in the titration with fluoride. This accounts for the formation of the band at 475 nm even before the addition of 1 equiv of F^-. In particular, with the addition of 1 equiv, 20% of the deprotonated form of **1** is present, which substantiates the detectable appearance of the band at 475 nm (see Figure 7c) and the orange nuance of the solution (see Figure 1).

Titration was carried out also with $[Bu_4N]Cl$, which induced the development of the band at 370 nm, as observed for previously mentioned oxoanions. No band development at higher wavelengths was detected also with the addition of a large excess of chloride. It is suggested that a hydrogen-bonding adduct, $[\mathbf{1}\cdot Cl]^-$, is formed, whose binding constant was calculated from the titration profile, log $K = 4.55 \pm 0.01$.

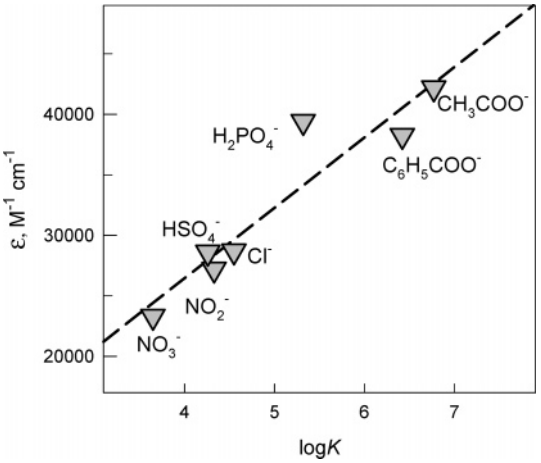

Figure 8. Linear correlation between the binding constants and the limiting absorbance at 370 nm for the $[\mathbf{1}\cdot anion]^-$ adducts in MeCN solution.

Thus, it appears that urea deprotonation is signaled by the appearance of a new absorption band at a long wavelength and takes place only in the case of fluoride. The F^- ion first establishes the strongest H-bond interaction with the receptor, as indicated by the highest value of log *K*. This is an expected behavior, in view of the high electronegativity of fluorine. Hydrogen-bonding interaction has been defined as an incipient proton-transfer process from the receptor to the anion.[10] F^-, among the investigated anions, induces the most pronounced "frozen" proton transfer from the urea subunit when added in a subequivalent amount. Indeed, a neat proton transfer takes place in the presence of a second equivalent of F^-. This is due to the particular stability of the $[HF_2]^-$ dimer, for which the highest hydrogen bond energy in the gas phase has been calculated (39 kcal mol^{-1}).[21] Thus, if *one* F^- ion is a fairly strong base in an MeCN solution, as documented by its ability to establish intense H-bond interactions with **1** and by the highest value of log K_1, *two* F^- ions represent a very strong base, capable of abstracting a proton from the urea subunit. It has to be noticed that the acidity of the urea moiety has been enhanced and its deprotonation favored due to the presence of two electron-withdrawing nitro substituents on the covalently linked phenyl rings.

With regard to the H-bond complexes between **1** and the oxoanions, a roughly linear relationship exists between log *K* and the limiting molar absorbance ϵ, as shown in Figure 8. The higher the energy of the H-bond interaction (expressed by log *K*), the higher the value of the molar absorbance of the complex.

To explain such an empirical relationship, one should consider that, on H-bond interaction with the anion, electron density is increased on each −NH fragment, thus strengthening the electrical dipole on each aromatic subunit of **1**. Thus, the band at 370 nm, resulting from the charge-transfer transition from the −NH fragment to the $-NO_2$ group, on each side of the chromophore, moves up with anion addition. The probability of the transition is related to the intensity of the dipole; the higher the dipole intensity (which is related to the H-bond interaction energy and to log *K*), the higher the probability of the transition and the value of the molar absorbance. Thus, the molar absorbance of the band at 370 nm gives a rather rough estimate of the intensity of the hydrogen-bonding interaction

(21) Gronert, S. *J. Am. Chem. Soc.* **1993**, *115*, 10258−10266.

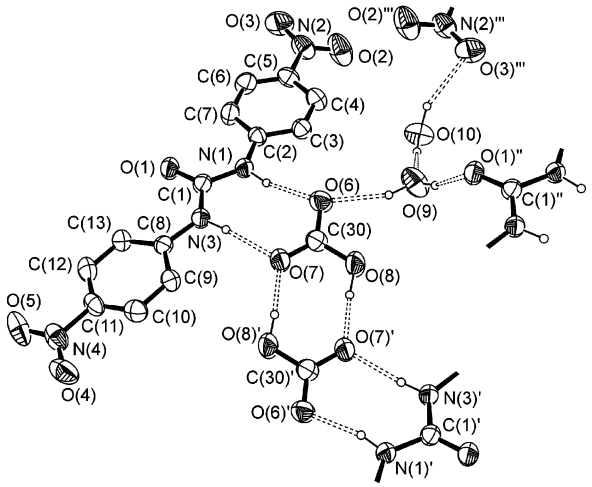

Figure 9. ORTEP view of the $[\mathbf{1}\cdot HCO_3]^-\cdot H_2O$ complex (thermal ellipsoids are drawn at the 30% probability level; only H atoms involved in intermolecular hydrogen bonds are drawn). Tetrabutylammonium ion has been omitted for clarity. Dashed lines indicate the hydrogen-bond interactions in the asymmetric unit and between symmetrically equivalent atoms. Symmetry codes: $(') = -x + 1, -y + 1, -z$; $('') = x + 1, y, z$; $(''') = -x + 1, -y + 1, -z + 1$.

and accounts for the approximately linear correlation between log K and ϵ. At this point, one could wonder about the behavior of the $[\mathbf{1}\cdot F]^-$ complex, which exhibits the highest log K value (log $K_1 = 7.38 \pm 0.09$), but whose absorbance is about one-half of that observed for acetate and dihydrogen phosphate complexes. We can tentatively suggest the following explanation: each investigated oxoanion (CH_3COO^-, $C_6H_5COO^-$, $H_2PO_4^-$, NO_2^-, HSO_4^-, and NO_3^-) forms with the urea subunit two N−H···O hydrogen bonds, from which two dipoles and two possible optical transitions originate. On the other hand, it is suggested that the small F^- ion specifically interacts with only one −NH fragment, thus strengthening only a single dipole, which justifies a reduced value of the molar absorbance. In contrast, chloride is well-behaving with respect to the ϵ/log K linear correlation, which suggests that the larger Cl^- anion establishes a bifurcated hydrogen-bonding interaction with the urea subunit of **1**, thus making the $[\mathbf{1}\cdot Cl]^-$ complex subject to two possible charge-transfer transitions. Unfortunately, we were not able to obtain crystals of $[\mathbf{1}\cdot Cl]^-$ to support this hypothesis on the basis of X-ray diffraction study. However, the crystal structure of the analogous complex, $[\mathbf{L}\cdot Cl]^-$ (L = 1,3-bis(4-chlorophenyl)urea), indicates bifurcated interaction of the chloride ion.[22]

Attempts were made to obtain crystals of the tetrabutylammonium salt of the deprotonated form of **1** with slow diffusion of diethyl ether into an MeCN solution containing the receptor and an excess of $[Bu_4N]F$. However, only a red oil separated. The red oil was redissolved in THF, and the solution was left to evaporate in open air. In a few days, yellow crystals of the salt, $[Bu_4N][\mathbf{1}\cdot HCO_3]\cdot 2H_2O$, were obtained, suitable for X-ray diffraction studies. Figure 9 shows the ORTEP diagram illustrating the molecular structure of the salt, which consists of a tetrabutylammonium cation, and of the anionic complex between **1** and HCO_3^-, with two molecules of water of crystallization. Apparently, the complex formed by reaction of

(22) Wamhoff, H.; Bamberg, C.; Herrmann, S.; Nieger, M. *J. Org. Chem.* **1994**, *59*, 3985−3993.

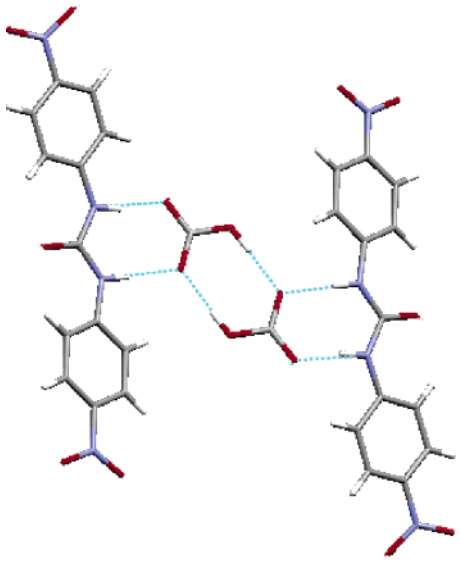

Figure 10. H-bond motif in the $\{[\mathbf{1}\cdot HCO_3]^-\}_2$ dimer. H-bonds have been drawn in light blue.

the deprotonated form of **1** (L^-) with carbon dioxide, in the presence of water, as illustrated by eq 2:

$$L^- + H_2O + CO_2 \rightarrow [LH\cdot HCO_3]^- \qquad (2)$$

It is seen that the 1,3-bis(4-nitrophenyl)urea framework is not perfectly planar, with dihedral angles between the N−CO−N group and the two phenyl rings of 3.5(1) and 7.8(1)°. Such a deviation, which is less pronounced than that observed in the $[\mathbf{1}\cdot CH_3COO]^-$ adduct, may also be ascribed to crystal packing effects, related to the presence of asymmetrically located water molecules.

More interestingly, the urea subunit of **1** gives a definite hydrogen-bonding complex with an HCO_3^- ion, with formation of two NH···O bonds. Moreover, each urea-bound HCO_3^- ion donates and accepts a hydrogen bond to/from another urea-bound HCO_3^- ion, giving rise to a dimer. A sketch of the H-bond dimer is shown in Figure 10. In particular, the O(7) atom, already involved in the interaction with the −NH fragment of the urea subunit, is also a proton acceptor for the OH···O interaction that occurs with the OH donor group of an adjacent HCO_3^-; thus, the two N−CO−N groups are linked via two hydrogencarbonate ions. This situation is common when urea and HCO_3^- are present; in particular, it occurs with very similar features in urea−hydrogencarbonate complexes, containing tetraethyl- or tetrabutylammonium as cations.[21] Relevant geometrical parameters related to the hydrogen-bonding interactions in the crystalline complex salt, $[Bu_4N][\mathbf{1}\cdot HCO_3]\cdot 2H_2O$, are shown in Table 2.

It has to be noted that NH···O interactions are weaker than those observed with the CH_3COO^- anion, as judging from the higher N··· O distance. This may be due to the fact that the acetate ion is solely involved in two H-bonds, while HCO_3^- further interacts with another HCO_3^-. Moreover, further H-bonds result from the presence of the water molecules in the crystal. The O(9) atom of the first water molecule is a proton donor for the O(6) atom of a hydrogencarbonate ion and for the O(1) carbonyl oxygen of an N−CO−N group, and then an HCO_3^- ion and a water molecule connect the donor −NH fragments and the acceptor carbonyl oxygen of two urea groups.

Finally, the O(10) of the second water molecule acts as a proton donor of OH···O interactions, with the O(9) atom of the first water molecule and with the O(3) atom of a nitro group.

Noticeably, it has been recently reported that in a 4-amino-1,8-naphthalimide-based receptor, the addition of excess F^- induced the deprotonation of the amino group, and that following fixation of atmospheric CO_2, an H-bond complex formed between the neutral receptor and HCO_3^-, according to an analogous mechanism.[23]

Conclusions

This investigation may represent a case study for the interaction of ureas with anions. Urea is an appropriate receptor for oxoanions because it can form two N−H···O bonds with two consecutive oxygen atoms of the anion. The interaction is essentially electrostatic, and its energy is related to the intrinsic basicity of the anion, whose magnitude can be evaluated, for instance, from the partial negative charge located on each oxygen atom of the anion. Thus, the sequence of log *K* values found in this work (CH_3COO^- > $C_6H_5COO^-$ > $H_2PO_4^-$ > NO_2^- > HSO_4^- > NO_3^-) corresponds to the *natural order*, to be observed in any urea-containing receptor in the absence of severe steric constraints, and ultimately determines the selectivity of anion recognition. Fluoride is a particular case as it has a size comparable to that of oxygen but holds an integral negative charge. Thus, among anions, F^- establishes the strongest H-bond interaction with an −NH fragment of the urea subunit. In particular, the interaction should correspond to an advanced stage of the proton transfer.[10] Indeed, proton transfer takes place in the presence of a second F^- ion, with formation of HF_2^-, the most-stable H-bond complex that fluoride can form. Just in view of the unique stability of HF_2^-, excess addition of fluoride should induce deprotonation of most urea derivatives, with the process being signaled by the appearance of a charge-transfer absorption band in the visible region and by a drastic color change. Despite the visual evidence, this feature has been missed in a recent report.[24]

Acknowledgment. The financial support of the European Union (RTN Contract HPRN-CT-2000-00029) and the Italian Ministry of University and Research (PRIN, Dispositivi Supramolecolari; FIRB, Project RBNE019H9K) is gratefully acknowledged.

Supporting Information Available: Crystallographic information (CIF) on the complex salts, $[Bu_4N][\mathbf{1}\cdot CH_3COO]$ and $[Bu_4N][\mathbf{1}\cdot HCO_3]\cdot 2H_2O$. This material is available free of charge via the Internet at http://pubs.acs.org.

JA045936C

(23) Gunnlaugsson, T.; Kruger, P. E.; Jensen, P.; Pfeffer, F. M.; Hussey, G. M. *Tetrahedron Lett.* **2003**, *49*, 8909−8913.

(24) Kwon, J. Y.; Yun Jung Jang, Y. J.; Kim, S. K.; Lee, K.-H.; Kim, J. S.; Yoon, J. *J. Org. Chem.* **2004**, *69*, 5155−5157.